# PMMA Adsorption Over Previously Adsorbed PS Studied by Polarized FTIR-ATR

ERWIN P. ENRIQUEZ, HILDEGARD M. SCHNEIDER, and STEVE GRANICK*

Department of Materials Science and Engineering, University of Illinois at Urbana-Champaign, Urbana, Illinois 61801

**SYNOPSIS**

Polarized infrared spectroscopy in attenuated total reflection was used to investigate the adsorption of PMMA (polymethylmethacrylate) onto PS (polystyrene) that was previously adsorbed onto oxidized silicon from dilute solution in carbon tetrachloride at 30°C. The carbonyl group of PMMA forms hydrogen bonds with surface silanol groups, giving segment–surface interaction energy of 4 $kT$ as against 1 $kT$ for PS ($k$ is the Boltzmann constant, $T$ the absolute temperature). The formation of hydrogen-bonding by PMMA was unaffected, in rate or amount, by preadsorbed PS, but a lesser total amount of PMMA adsorbed onto PS, resulting in a higher average bound fraction. The histogram of the mass adsorbed, attributable to subpopulations of chains with different bound fractions, was inferred by subtracting infrared spectra acquired at successive times. Whereas this histogram was broad and bimodal for adsorption onto bare surface, it was narrower and unimodal for adsorption onto preadsorbed PS. © 1995 John Wiley & Sons, Inc.

**Keywords:** Surface • adsorption • exchange • FTIR-ATR • histogram • hydrogen-bond

## INTRODUCTION

Many of the physical chemical properties of flexible polymers (in solutions, blends, melts, and adsorbed layers) are governed by conformational freedom of the chains.[1,2] Upon localization at an interface, constraints to conformational relaxations occur, particularly for the bound segments (trains). Therefore, depending upon the strength of segment-surface interaction ($\chi_s$) and chain flexibility, equilibration of the adsorbed layer at the interface may be very slow, especially for large $\chi_s$.[2-7] Recent experimental findings, based upon analysis of equilibration kinetics, point to persistent metastable states in adsorbed layers.[2-6] To date, understanding of the complex factors that determine the structure and properties of unequilibrated adsorbed polymers is still incomplete,[3] in part because of the low mass involved, typically only 1–3 mg/m$^2$ for adsorption from dilute solutions. The paucity of experimental probes that are directly sensitive to the structure of such small quantities has limited advances in this area.

We investigate here the effect of a preadsorbed polymer layer on the infrared dichroism and the adsorption kinetics of a second polymer that displaces the former from the interface. We are interested to compare how the bare substrate and one that is initially covered by a weakly adsorbed polymer, differ in how they present themselves to an adsorbing polymer. One might expect the presence of preadsorbed polymer to present a different barrier and different interfacial properties than the bare surface. This scenario is ubiquitous in nature, where most adsorption processes involve multicomponent systems. Examples include soils, interfacial proteins, and multifarious other colloidal systems.

The system was preadsorbed deuterio polystyrene (PS-d), adsorbed onto a single solid surface of oxidized silicon from dilute solution in carbon tetrachloride ($CCL_4$), and displaced by polymethylmethacrylate (PMMA). The stronger segment-surface interaction energy $\chi_s$ for PMMA ($\chi_s$ ca. 4) than for PS ($\chi_s$ ca. 1) promoted the exchange process at the oxidized silicon surface.[8-11] Previous studies on this same system showed that the desorption of PS fol-

* To whom correspondence should be addressed.

Journal of Polymer Science: Part B: Polymer Physics, Vol. 33, 2429–2437 (1995)
 CCC 0887-6266/95/172429-09

lowed a rate that was diffusion-limited, consistent with stretched exponential kinetics, with non-Arrhenius dependence on temperature.[8]

In efforts to follow the structure of the evolving polymer layer, we now use polarized rather than unpolarized infrared radiation, employing an apparatus that was described recently.[13] This allowed us to monitor average segmental orientations at the interface in addition to the overall kinetics of the adsorption and exchange process. Control experiments involved adsorption of PMMA onto the initially bare surface.

## EXPERIMENTAL

### Materials

The two polymer samples were purchased from Polymer Laboratories. The PMMA (atactic) had weight-average molecular weight $M_w$ = 400,000 g-mole$^{-1}$ and ratio of weight to number-average molecular weight $M_w/M_n$ = 1.10. The PS-d (atactic) had $M_w$ = 550,000 g-mole$^{-1}$ and $M_w/M_n$ = 1.05). The solvent, spectroscopic grade carbon tetrachloride (Fisher), was used as received.

The flat plate, 45° trapezoidal Si ATR prism, was obtained from SpectraTech. The sequence of surface pretreatment prior to every adsorption experiment consisted of the following: (1) Ultrasonication of the ATR prism in ethyl acetate bath for about 10 min, followed by rinse with deionized, glass-distilled water, (2) treatment with 5% hydrofluoric acid for about 1 min, followed by Nanopure water rinse and $N_2$ gas blow drying, (3) plasma treatment with $O_2$ gas for 5 min, followed by a 5 min cooling period under low oxygen pressure. This protocol was found to reproducibly yield the same oxidized silicon surface for polymer adsorption experiments; details of the preparation and comparison with alternative methods were reported previously.[14] The Fourier transform infrared (FTIR) spectrometer was a Biorad FTS-60A equipped with a mid-IR range mercury cadmium telluride detector. A wire-grid polarizer (Graesby/Specac) was positioned between the infrared beam path and the sample cell, and could be switched intermittently between $p$- and $s$-polarization settings during the experiment. Absorbance spectra were referenced to the background solvent spectrum obtained separately for each polarization setting. Adsorption experiments were done at 30.0°C in a stainless steel thermostated cell.

Figure 1 shows a schematic representation of the adsorption cell. Its geometry is shown in the top panel. The coordinate system for analysis of measurements employing polarized radiation is shown in the bottom panel.

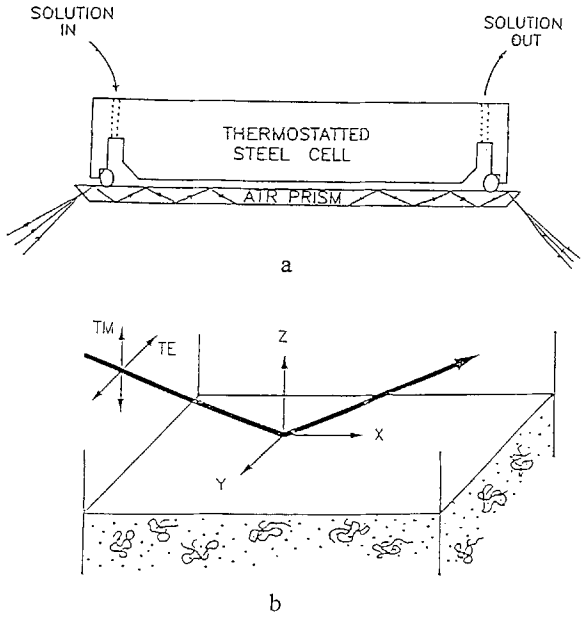


**Figure 1.** Schematic representation of the adsorption cell (a) and of the laboratory coordinate system (b). The $p$-polarization direction (transverse magnetic, TM) corresponds to the electric field vector of the incident that is parallel to the plane of incidence. With respect to the substrate coordinate axes ($x$, $y$, $z$), the TM component will have components along the $x$-$z$ plane. The $s$-polarization (transverse electric, TE) is perpendicular to the plane of incidence, and has a component only in the $y$ direction.

### Data Acquisition and Analysis

Interferograms were collected intermittently for $p$- and $s$-polarization setting, averaging 64 scans (which took ≈0.5 min at 8 cm$^{-1}$ resolution) for the first 5 min, 128 scans (ca. 1 min) for the next 10 min, and then 512 (ca. 2.5 min) scans for the remainder of the experiment. The interferograms were processed later into single beam spectra and ratioed to the background spectrum to obtain the final absorbance spectra. Thus, a sequence of semicontinuous time-averaged data were acquired. After about 1 min into the experiment, increasing the number of scans did not significantly affect the ratio of signal to noise.

Raw data are illustrated in Figure 2. Absorbance is plotted against wavenumber for $p$-polarized radiation (top panel) and $s$-polarized radiation (middle panel). The dichroism implied from comparison of these two polarizations (bottom panel) is discussed below.

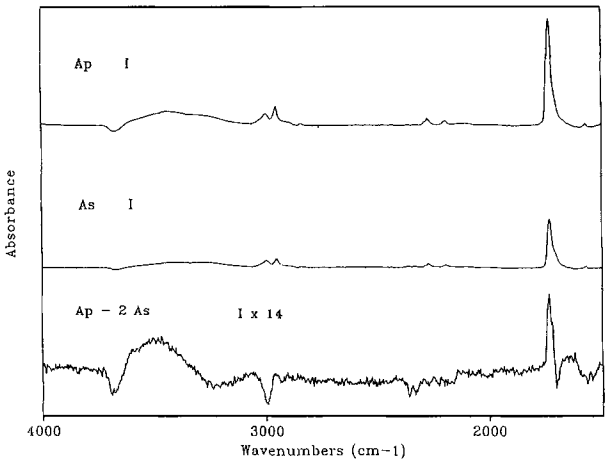


**Figure 2.** Examples of infrared absorbance spectra obtained during the exchange process (130 min after of exchange of PS-d for PMMA solution). Top: parallel polarization. Middle: perpendicular polarization. Bottom: the difference spectrum, $A_p - 2A_s$, showing average anisotropy in the silanol O–H stretches and the $\nu_a$ $CH_3$ and C=O vibrational modes of PMMA (see text). The ordinate scale, in the bottom panel, is enlarged by a factor of 14. Data concern adsorption of PMMA from concentration 0.01 mg/mL in $CCl_4$.

Figure 3 shows examples of the curve-fitting. The purpose was quantitative analysis; fitting of the curves, rather than obtaining physically fundamental fits, was the goal. The carbonyl band of PMMA (Fig. 3A), at 1732 $cm^{-1}$, was empirically resolved into two Gaussian components centered at 1732 $cm^{-1}$ (free carbonyl) and 1714 $cm^{-1}$ (bound carbonyl)[5,15] by a nonlinear least-squares fitting routine; the peak centers and bandwidths were not fixed, and a baseline correction was incorporated (Fig. 3). The two peak centers were found to be stable with time with standard deviation of $\pm 1$ $cm^{-1}$. Similarly, the C–D stretch region of PS-d (2000–2400 $cm^{-1}$) and the C–H stretch region (2780–3120 $cm^{-1}$) of PMMA were resolved into several Gaussian component peaks. The PMMA C–H bands were fitted with 8 component peaks; the two leftmost bands in Figure 2B constitute the asymmetric methyl stretch. The centers of these components were not fixed in the curvefitting routine and were also found to be stable to $\pm 1$ $cm^{-1}$.

Examples of the integrated peak intensities, obtained in *p*- and *s*-polarizations, are shown in Figures 4 and 5 (discussed below). Since these data were not acquired at precisely the same times, it was necessary to interpolate the data for comparison. To do this, the raw data were fitted with empirical functions (double or triple exponentials) by nonlinear least-squares fits using the Marquardt-Levenberg algorithm.[16] In Figure 4, the dotted lines are these fits. Typical coefficients of determination were better than 0.95.

For an isotropic absorbing system, $A_p/A_s = 2$ since $A_p$ samples two directions in the rarer medium, and $A_s$ a single direction. Because *p*-polarization samples two directions of space, the isotropic solution contributes an oscillator density proportional to $(\frac{2}{3})$ the solution concentration. Similarly, because *s*-polarization samples a single direction of space, the isotropic solution contributes an oscillator density proportional to $(\frac{1}{3})$ the solution concentration.

It was therefore convenient to plot the quantity $(A_p - 2A_s)$ as a qualitative indicator of whether dichroism existed. An example is shown in Figure 2 (bottom). One observes obvious dichroism of PMMA bands (asymmetric $CH_3$ and C=O stretching vi-

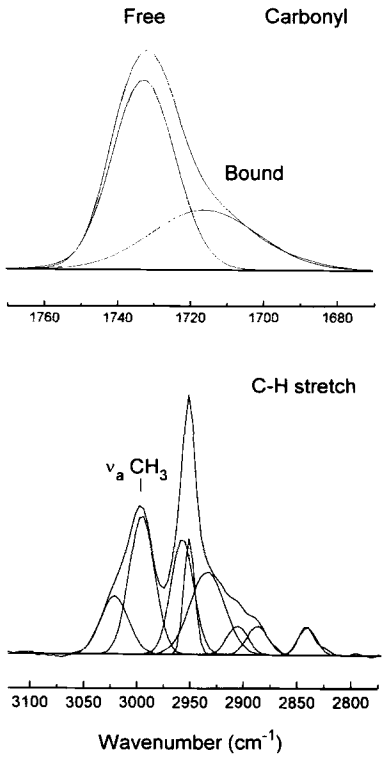


**Figure 3.** The carbonyl (top panel) and C–H stretching regions (bottom panel) of PMMA, showing the Gaussian peaks used to fit the spectral bands empirically. The carbonyl stretching frequency was resolved into free and hydrogen-bonded components. The latter was shifted to lower frequency with absorptivity ca. 1.5 times that for the free carbonyl.[15] No fundamental significance is attributed to the numerous peaks used for curve-fitting in the C–H stretch region.

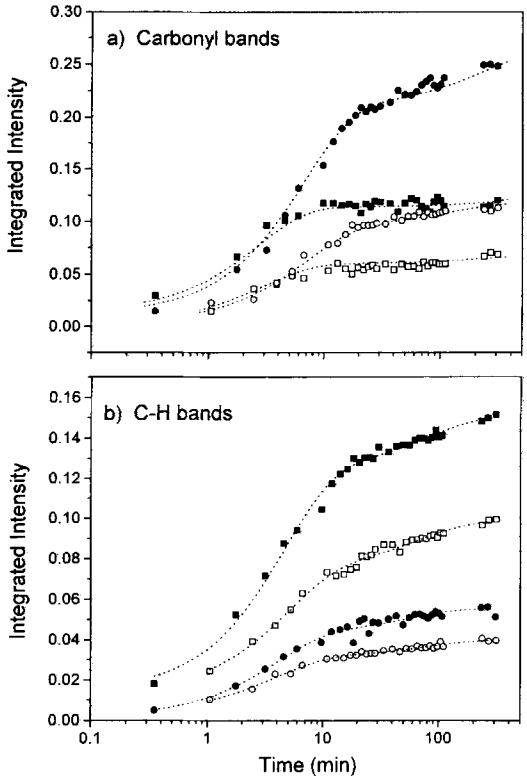


**Figure 4.** Representative absorbance data for *p*- (solid symbols) and *s*-polarization (open symbols) in a semi-log plot against time: (a) carbonyl bands (circles denote free, squares denote bound), (b) C–H bands (circles denote $\nu_a$ $CH_3$, squares denote sum of all C–H stretches). Adsorption is onto the initially bare solid surface from concentration 0.01 mg/mL in $CCl_4$.

brations) but not of PS-d, whose C–D vibrations apparently carried no net orientation.

The integrated intensities were converted to surface excess (mass adsorbed per area) after the solution contribution to the signal was subtracted. The solution calibration was calibrated from the ATR intensity of PMMA solutions in contact with a nonadsorbing surface. The nonadsorbing surface was the ATR prism coated with a self-assembled monolayer of OTE, octadecyltriethoxysilane[18]). Conversion of the infrared absorbance to mass adsorbed was calculated as previously reported for experiments involving unpolarized radiation,[5,19] with the difference being that a differing abundance of oscillators contributes to the ATR signal in the case of polarized radiation.

A typical experiment proceeded by first allowing PS-d to adsorb from 1.0 mg/mL solution in $CCl_4$ for about 40 min. This was then followed by replacement of PS-d solution for one of PMMA (0.010 mg/mL or 0.050 mg/mL). As previously reported,[8] no dependence on time lag between exchange of solutions was observed.

A typical exchange experiment is depicted in Figure 5; the effective surface excess in the two polarization directions is plotted. The total surface excess, plotted against time in Figure 6, is the sum of these quantities.

On the time scales of these plots, the PS-d reached a steady-state mass adsorbed almost immediately. About 40 min into the experiment, the solution was replaced with PMMA and slow desorption of PS-d was observed, concurrent with adsorption of PMMA.

## RESULTS AND DISCUSSION

### PMMA Adsorption onto Initially Bare Surface

Figure 6 compares the time evolution of the total mass adsorbed ($\Gamma$) and the mass of hydrogen-bonded segments of PMMA through the carbonyl groups ($\Gamma_{bound}$) onto the initially bare surface and onto previously adsorbed PS-d. The time scale is logarithmic in order to emphasize changes at long times. Two PMMA dilute solution concentrations are contrasted: $c_1$ = 0.010 mg/mL and $c_2$ = 0.050 mg/mL.

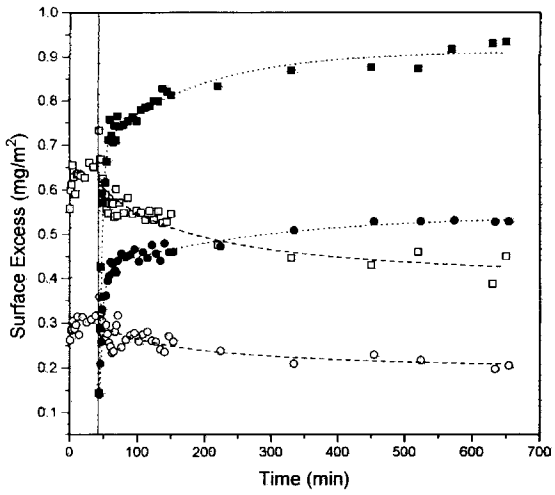


**Figure 5.** Surface excess in the two polarization directions for PS-d (open symbols, 1 mg/mL) and PMMA (solid symbols, 0.01 mg/mL) during the exchange process. The total surface excess is the sum of this value in *p*-polarization (squares) and in *s*-polarization (circles). Because the *p* and *s* data were not obtained at the same times, empirical fits to the data points (dotted and dashed lines) were used to calculate the total surface excess values and the dichroic ratios. Adsorption was onto the initially bare solid surface from concentration 0.01 mg/mL in $CCl_4$.

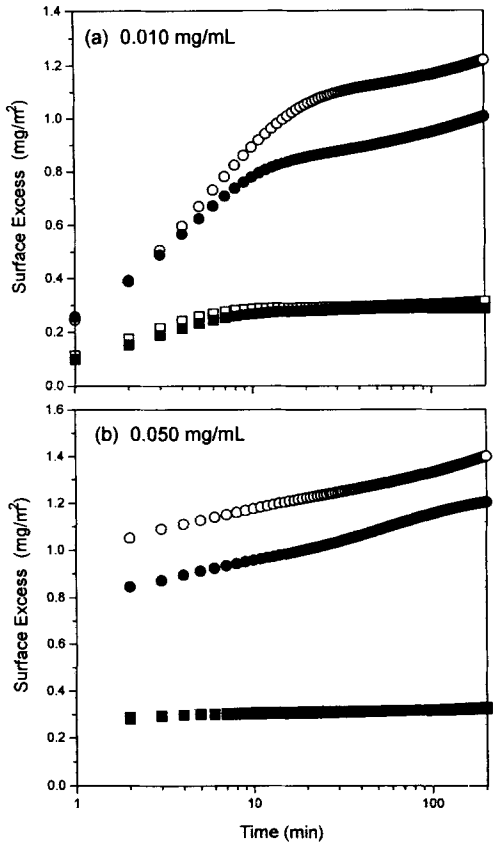


**Figure 6.** Total PMMA surface excess ($\Gamma$) and bound carbonyl surface excess ($\Gamma_{bound}$) plotted against logarithmic time for adsorption from two solution concentrations as indicated in the graph. Adsorption was onto an initially bare substrate and onto preadsorbed PS-d. For both concentrations, the legend is: open circles, $\Gamma$ onto bare substrate; filled circles, $\Gamma$ for PS-d exchange; open squares, $\Gamma_{bound}$ onto bare substrate; filled squares, $\Gamma_{bound}$ for PS-d exchange.

For the more dilute solution, one observes an initial rise of mass adsorbed for about 10 min, followed by a regime of slower adsorption. The initial rise reflected a period during which adsorption was rate-limited by diffusion of chains through solution to the surface. Indeed, the data for the first 10 min grew in proportion to $t^{1/2}$ ($t$ is elapsed time). Assuming steady state, center of mass diffusion of the polymer chains, this implies that the diffusion coefficient of this PMMA in $CCl_4$ was roughly $2 \times 10^{-11}$ $m^2/s$ at 30°C, which is consistent with reported values.[14]

For both $c_1$ and $c_2$ experiments involving adsorption onto the initially bare substrate, the rate of adsorption slowed when $\Gamma$ ca. 0.8 mg/m$^2$ was reached, and ensuing kinetics were consistent with logarithmic dependence on time (see below). The point is that diffusion-limited adsorption discussed above could only continue to a finite surface coverage. After a certain coverage was attained, the nature of subsequent mass arrival was affected by the presence of other chains and the scarcity of surface sites in general. We speculate below on the mechanism of the adsorption of these late-arriving chains.

## PMMA Adsorption Over Previously Adsorbed PS

Figure 6 also allows us to compare adsorption onto a bare substrate with adsorption during an exchange experiment. Obvious from the data showing the hydrogen-bonded mass is that the presence of the previously adsorbed PS hardly perturbed the PMMA, at least initially. PMMA interacts much more strongly than PS with the surface ($\chi_s = 4$ for PMMA and $\chi_s = 1$ for PS), and apparently PMMA-silanol interactions dominated until silanols are nearly saturated. At longer times, when most of the silanol groups were occupied, a significant disparity in the total mass of PMMA adsorbed becomes apparent when comparing the adsorption onto bare substrate with that over PS. The kinetics of the continuing PMMA adsorption at long times, however, are not really dissimilar, indicating that the effect of PS on *mass adsorbed* is stronger than the effect on adsorption rate.

Figure 7 plots the same data in a more common, linear fashion. It is again stressed that the plateau level of PMMA adsorbed during an exchange experiment was lower due to the continued presence of lingering PS. Long-time kinetics again show that small amounts of PMMA continued to arrive at the surface, and that the rate of mass deposition was only slightly larger than onto an initially bare surface. At long times the adsorption was a symmetric flux between adsorbing PMMA and desorbing PS-d. This we also observed in another system.[27] The phenomenon appears to be a consequence of slowly equilibrating layer composition.[27] In the mixed interface, the total polymer concentration was roughly 30% higher than for adsorption of PMMA onto the initially bare surface.

## Kinetics of PMMA Adsorption

The mechanism of continued growth in surface excess at long times is, at present, not clearly understood. Predictions of logarithmic time dependence which we encounter have been advanced by de Gennes[29] and Joanny and Semenov.[30] In those the-

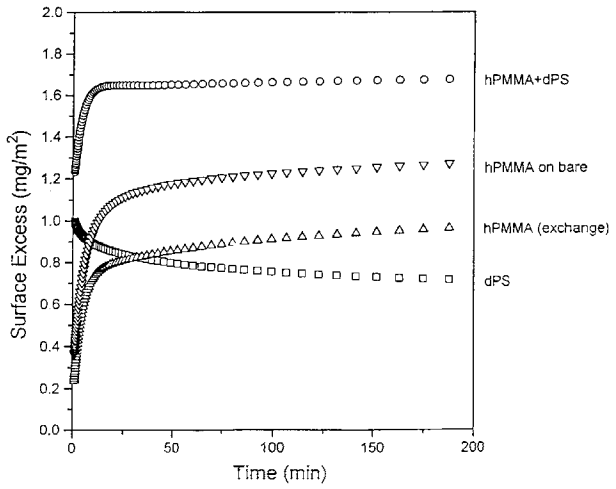


**Figure 7.** Comparison of time dependence of the surface excess for adsorption onto a bare surface and after exchange of PS-d solution for PMMA solution (0.010 mg/mL). Plotted are the total surface excess (PMMA plus PS-d) during the exchange experiment (circles), the surface excess of PMMA adsorbed onto the bare surface (inverted triangles), the surface excess of PMMA adsorbed onto preadsorbed PS-d (triangles), and the surface excess of PS-d during displacement by PMMA (squares).

ories, end-in reptation is considered to be the mechanism of chain entry into an almost saturated monolayer. While this scenario may satisfy one's intuitive picture of adsorption at an initially bare substrate, concurrent PS desorption during an exchange experiment complicates this. In the exchange experiment where PS continually desorbs, the adsorption of PMMA in the pseudo-plateau at long times was slightly enhanced as compared to adsorption at a bare surface. The PS desorption followed stretched exponential kinetics, corroborating previous findings;[8,20,21] the phenomenon is believed to be controlled by the steric restrictions imposed by the surrounding PMMA chains. As the adsorption and the desorption kinetics during the exchange appear to be interdependent, simple end-in reptation is likely not the only mechanism one should consider.

## Adsorbed Layer Structure

To better understand the events at the surface, consider what can be deduced about the structure of the layer as it evolved. Figure 8 shows the evolution of the average bound fraction of the PMMA adsorbed for both adsorption and exchange experiments. Subtle differences now appear, especially at the extremes of surface coverage. Early in time, when the surface coverage was low, one notices the high bound fraction of 0.45, implying that the chains were highly flattened. When chains adsorbed onto a layer of previously adsorbed PS, however, the bound fraction was somewhat lower, around 0.4, indicating that the PS chains slightly inhibited the flattening of PMMA at the surface. At long times, as the layer became saturated, one notices that the average bound fraction of the chains adsorbing onto bare silicon fell below that of the PMMA at the mixed polymer interface. The situation becomes clearer when one considers Figure 9, which plots the bound fraction evolution as a function of the total PMMA mass adsorbed.

Figure 9 supports our supposition that chains at a bare surface were flatter than those arriving when PS is already present, and one is cautioned to recall that while equivalent quantities of PMMA are shown in this graph, considerable amounts of PS were also present in the exchange experiments. This is important when considering the bound fraction at which PMMA adsorption became appreciable. In the case of adsorption at a bare surface, Figure 6 shows that total PMMA adsorbed was much greater than that over a layer of PS. Late-arriving chains in the adsorption experiment with pure PMMA caused the average bound fraction to fall, indicating looser binding. This loosely bound PMMA was not evident in the case of the exchange experiment, perhaps because the surface sites required for that ad-

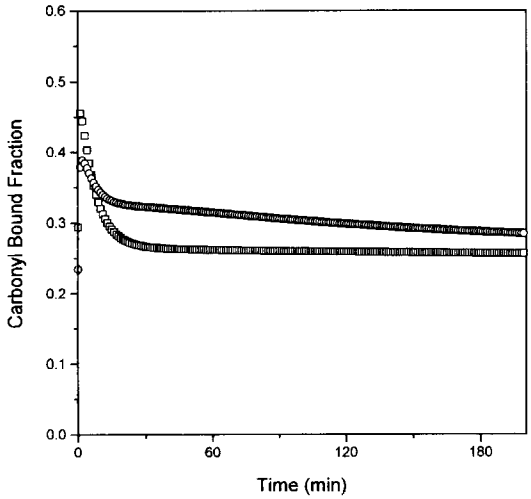


**Figure 8.** PMMA carbonyl-bound fraction plotted against time elapsed for the experiments displayed in Fig. 6 at 0.010 mg/mL: squares, onto bare substrate; circles, exchange with PS-d.

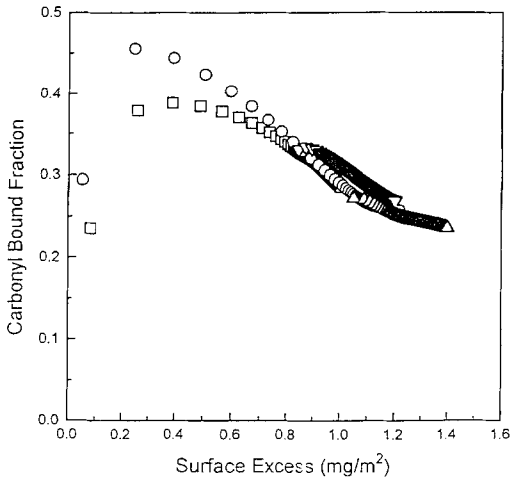


**Figure 9.** Carbonyl-bound fraction plotted against surface excess of PMMA for the adsorption conditions of Fig. 6: circles, 0.010 mg/mL, onto bare substrate; squares, 0.010 mg/mL, for PS-d exchange; inverted triangles, 0.050 mg/mL, onto bare substrate; triangles, 0.050 mg/mL, for PS-d exchange.

sorption were already occupied by PS, which was slow to desorb.

Earlier experiments by Schneider and Frantz[26] have quantified the apparently heterogeneous adsorption states within a layer of PMMA. The key point necessary for the analysis is the assumption, validated by Frantz et al.,[21] that the bound fraction of PMMA chains does not change after adsorption. This lack of relaxation results in a broad distribution of bound fractions within the adsorbed layer; the bound fraction appears to depend on the surface silanol availability at the time of chain arrival. The chains which arrived at low surface coverage possessed the higher bound fraction; the chains that arrived at high surface coverage possessed the lower.

With this same assumption of lack of conformational rearrangement, the distribution of bound fraction was quantified by subtracting infrared spectra acquired at successive times. Figure 10 compares the resulting distribution of bound fraction, for both adsorption onto the initially bare surface and adsorption onto PS.

For adsorption at the initially bare surface, one observes a subpopulation of more highly flattened chains (higher bound fraction) than when PS blocked some of the surface sites. Once these sites (the surface silanols) had saturated, the subsequently arriving PMMA chains were forced into looser binding states (lower bound fraction). The bimodal distribution depicted for adsorption onto a bare surface agrees well with that discussed by Schneider and Frantz.[26]

The distribution of adsorbed PMMA over the initially adsorbed layer of PS shows provocative differences. Not only were the initially arriving chains prevented from spreading to the higher bound fraction ($p$ = 0.45), but the presence of PS prevented the "loose" layer growth which occurred otherwise at long times. It is tempting to imagine, from the differences in the distributions in Figure 10, that the PS initially at the surface was forced into the "looser" conformations missing in the second PMMA distribution. This is plausible as differences in $\chi_s$ indicate that the hydrogen-bonding interaction of PMMA with surface silanols is four times stronger than the weak association of PS with the surface. It does, however, complicate the picture of slow PS desorption. Initial work from this laboratory postulated that PS desorbed slowly because it was trapped under a PMMA overlayer.[20] With bound fractions on the order of 0.4, however, it is hard to imagine loop sizes large enough to "staple" PS to the surface.

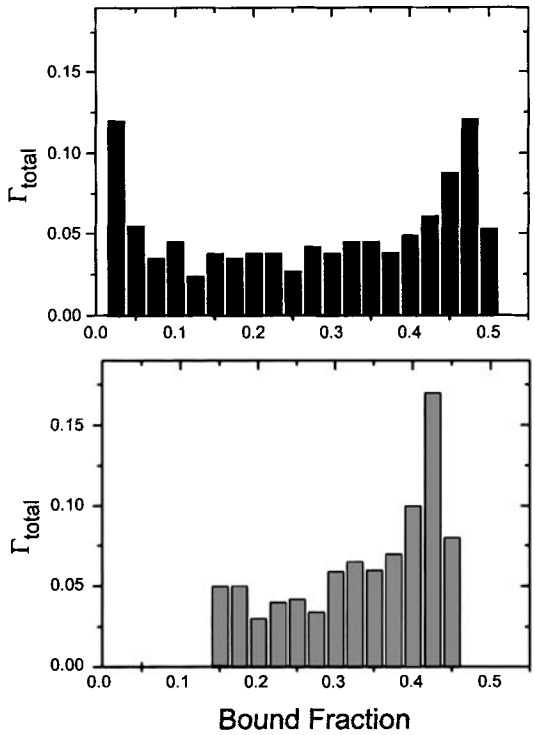


**Figure 10.** Histograms of carbonyl-bound fraction in adsorbed layers of PMMA at bare silicon oxide (top) and onto preadsorbed PS (bottom). Histograms evaluated at surface coverages 1.00 and 0.86 mg/m$^2$, respectively. The PMMA adsorbed from 0.010 mg/mL solution in both cases.

Two speculative possible scenarios come to mind. Perhaps as PMMA flooded the surface, PS chains aggregated and collapsed to minimize contact with the surrounding PMMA. While this picture might explain the observed slow and tortured PS desorption, it would not account for the lack of inferred difference in the subpopulation of PMMA at high bound fraction (Fig. 10). If PS segregated into collapsed islands, less PMMA should be able to flatten, and the distribution should be skewed toward looser binding (fewer silanols available).

As only the subpopulation of PMMA at lower bound fraction was perturbed, a different possibility suggests itself. Imagine that as surface sites were stolen from PS by incoming PMMA, the portions of PS chains not attached to the surface as trains became extended away from the surface, leaving the PMMA chains free to adsorb in a manner not measurably different from adsorption onto the bare surface. It is only when most of the contiguous surface silanols were already occupied by PMMA that the PS measurably perturbed the PMMA structure. At this stage, the end-in reptation required to form a saturated PMMA layer would be complicated by the necessity for PS chains to desorb through a layer of PMMA, with which the enthalpic interactions are unfavorable. Experiments show that the PS desorption is very slow; therefore the PMMA adsorption also slowed, with the result that the loosely bound population of PMMA is almost entirely missing.

But at very long times (longer than the experiments lasted), one expects PS to desorb completely and that the adsorbed mass of PMMA would likely reach the same level as for adsorption onto a bare substrate. Then the distributions of bound fraction (Fig. 10) would be identical.

### Dichroism Studies

This work was conducted with polarized FTIR in the hope of inferring the chain orientations relative to the solid surface. Previous work[21] showed that the asymmetric methyl stretch of PMMA acquires preferred orientation parallel to the plane of the infrared crystal. Our measurements confirmed those observations. Unfortunately, PS-d vibrations were too small to give reliable dichroic information and the PMMA vibrations which exhibited reliable dichroism were limited to the side-chain methyl and carbonyl units already described.[21] While these moieties did display signs of being constrained to preferred average orientations, especially in chains whose bound fraction was high, they afforded no direct insight into the orientation of the polymer backbone itself. Future investigations from this laboratory will emphasize chains in which the *backbone* vibrations exhibit dichroism.[32] In the present study, the bound fraction and its histogram remain the reliable source of conformational information.

We are grateful to Svetlana Sukhishvili and Ali Dhinojwala for help and discussions. Support was provided through the National Science Foundation (Polymers Program), Grant NSF-DMR-91-01509.

## REFERENCES AND NOTES

1. P. Flory, *Introduction to Polymer Chemistry,* Cornell University Press, Ithaca, NY, 1953.
2. P.-G. de Gennes, *Macromolecules,* **13,** 1069 (1980).
3. S. Granick, in *Physics of Polymer Surfaces and Inteface,* I. C. Sanchez, ed., Butterworth-Heinemann, Boston, 1992.
4. H. E. Johnson and S. Granick, *Macromolecules,* **23,** 3367 (1990).
5. P. Frantz and S. Granick, *Macromolecules,* **27,** 2553 (1994).
6. J. S. S. Schaffer and A. K. Chakraborty, *Macromolecules,* **26,** 1120 (1993), and references cited therein.
7. G. J. Fleer, M. A. Cohen Stuart, J. M. H. M. Scheutjens, T. Cosgrove, and B. Vincent, *Polymers at Interfaces,* Chapman and Hall, London, 1993.
8. H. E. Johnson and S. Granick, *Science,* **255,** 966 (1992); H. E. Johnson, J. F. Douglas, and S. Granick, *Phys. Rev. Lett.,* **70,** 3267 (1993).
9. C. Thies, *J. Phys. Chem.,* **70,** 3783 (1966).
10. K. Kobayashi, A. Dochi, H. Yajima, and R. Endo, *Bull. Chem. Soc. Jpn.,* **66,** 1938 (1993).
11. I. D. Robb and R. Smith, *Polymer,* **18,** 500 (1977).
12. P. Frantz and S. Granick, *Macromolecules,* in press.
13. N. J. Harrick, *Internal Reflection Spectroscopy,* Interscience, New York, 1967.
14. P. Frantz and S. Granick, *Langmuir,* **8,** 1176 (1992).
15. The bound carbonyl has ca. 1.5 times higher infrared absorptivity than the free carbonyl, as first reported by M. Coleman and P. Painter. *Appl. Spectrosc. Rev.,* **20,** 255 (1985).
16. In the software ORIGIN. See also, P. Gans, *Data Fitting in the Chemical Sciences,* Wiley, New York, 1992.
17. P. A. Fluornoy and W. J. Schaffers, *Spectrochimica Acta,* **22,** 5 (1966).
18. J. Peanasky, H. M. Schneider, S. Granick, and C. R. Kessel, *Langmuir,* **11,** 953 (1995).
19. R. P. Sperline, S. Muralidharan, and H. Freiser, *Langmuir,* **3,** 198 (1987).
20. J. Douglas, H. E. Johnson, and S. Granick, *Science,* **262,** 2010 (1993).
21. P. Frantz and S. Granick, *Macromolecules,* in press.

22. P. Schaaf and J. Talbot, *Phys. Rev. Lett.*, **62,** 175 (1989); P. R. Van Tassel, P. Viot, G. Tarjus, and J. Talbot, *J. Chem. Phys.*, **101,** 7064 (1994).
23. J. J. Ramsden, *Phys. Rev. Lett.*, **71,** 295 (1993).
24. R. K. Iler, *The Chemistry of Silica,* Wiley, New York, 1979.
25. M. L. Hair, *J. Colloid Interface Sci.*, **59,** 532 (1977).
26. H. M. Schneider, P. Frantz, and S. Granick, submitted.
27. H. M. Schneider, S. Granick, and S. Smith, *Macromolecules,* **27,** 4714 (1994); *ibid,* 4721.
28. C. P. Tripp and M. L. Hair, *Langmuir,* **9,** 3523 (1993).
29. P. G. de Gennes, in *Molecular Conformation and Dynamics of Macromolecules in Condensed Systems,* M. Nagasawa, ed., Elsevier, Amsterdam, 1988; P. G. de Gennes, in *New Trends in Physics and Physical Chemistry of Polymers,* L.-H. Lee, ed., Plenum, New York, 1989.
30. J.-F. Joanny and A. F. Semenov, submitted.
31. The average tilt angle from the surface normal is $\int \theta \sin\theta \, d\theta$ for a hemispherical (isotropic) distribution of $\theta$ at the surface.
32. E. Enriquez and S. Granick, unpublished results.
33. M. Urban, *Vibrational Spectroscopy of Molecules and Macromolecules on Surfaces,* Wiley, New York, 1993.
34. K. Schmidt-Rohr, A. S. Kulik, H. W. Beckham, A. Ohlemacher, U. Pawelzik, C. Boeffel, and H. W. Spiess, *Macromolecules,* **27,** 4733 (1994).
35. J. C. Dijt, M. A. Cohen Stuart, and G. J. Fleer, *Macromolecules,* **25,** 5416 (1992).

*Received May 1, 1995*
*Revised July 12, 1995*
*Accepted July 27, 1995*